

# The albedo dichotomy of Iapetus measured at UV wavelengths

Amanda R. Hendrix <sup>\*</sup>, Candice J. Hansen

*Jet Propulsion Laboratory, California Institute of Technology, Mail Stop 230-250, Pasadena, CA 91109, USA*

Received 12 February 2007; revised 19 July 2007

Available online 21 September 2007

## Abstract

The dramatic hemispheric dichotomy in albedo displayed by Saturn's moon Iapetus has intrigued astronomers for centuries. Here we report on far-ultraviolet observations of Iapetus' bright and dark terrains from Cassini. We compare the reflectance spectra of Iapetus' dark terrain, Hyperion and Phoebe and find that both Phoebe and Hyperion are richer in water ice than Iapetus' dark terrain. Spectra of the lowest latitudes of the dark terrain display the diagnostic water ice absorption feature; water ice amounts increase within the dark material away from the apex (at 90° W longitude, the center of the dark leading hemisphere), consistent with thermal segregation of water ice. The water ice in the darkest, warmest low latitude regions is not expected to be stable and may be a sign of ongoing or recent emplacement of the dark material from an exogenic source.

© 2007 Elsevier Inc. All rights reserved.

*Keywords:* Ices, UV spectroscopy; Iapetus; Satellites, composition; Saturn, satellites; Ultraviolet observations

## 1. Background

Iapetus has intrigued planetary scientists for centuries, primarily due to its striking hemispheric albedo dichotomy. The leading hemisphere (centered on 90° W) is very dark, reflecting just ~4% of the visible light that hits it, while the trailing hemisphere (centered on 270° W), is relatively quite bright and has a visible albedo of ~60%. In this report, we present the first far-UV (1100–1900 Å) observations of Iapetus. First we briefly discuss results from previous Iapetus studies at longer wavelengths.

A long-standing question has been whether Iapetus' leading hemisphere dark terrain was created through exogenic processes (Cook and Franklin, 1970) or whether geologic activity emplaced dark material from within Iapetus (Smith et al., 1981, 1982). Voyager images of dark-floored craters within the bright terrain pointed to an endogenic source; they also suggested that the bright-dark boundary is too irregular to be consistent with infalling dust (Smith et al., 1981, 1982). However, albedo patterns observed by Cassini cameras in late 2004 suggest external emplacement of material (e.g., dark mater-

ial on ram-facing crater walls at high latitudes) (Porco et al., 2005). The initial theory of an exogenically-created dark pattern (Cook and Franklin, 1970) suggested that pre-existing dark material was uncovered by meteoritic bombardment; this idea was extrapolated upon by Wilson and Sagan (1996). Later researchers theorized (Soter, 1974) that the dark material is exogenically emplaced on Iapetus' leading hemisphere as material is lost from the moon Phoebe (Burns et al., 1979). Retrograde Phoebe dust from 215 R<sub>S</sub> would travel inward and impact the leading hemisphere of Iapetus, orbiting at 59 R<sub>S</sub>. However, Phoebe is spectrally gray at visible wavelengths, while the Iapetus dark material is reddish (Cruikshank et al., 1983; Squyres et al., 1984). If the material does come from Phoebe, then some sort of chemistry or impact volatilization must occur to change the color and darken the material (Cruikshank et al., 1983; Buratti and Mosher, 1995). Another possibility is that the exogenic source of the dark material is either Hyperion (Matthews, 1992) or Titan (Wilson and Sagan, 1995). Matthews (1992) suggested that the impact that disrupted Hyperion created a debris cloud that subsequently impacted Iapetus. Both Hyperion and Titan tholin material are spectrally reddish (Thomas and Veverka, 1985; McDonald et al., 1994; Owen et al., 2001), though not as dark as Iapetus. Buratti et al. (2002, 2005a) suggested that both Hyperion and Iapetus' leading hemispheres are impacted by dark, reddish dust from

<sup>\*</sup> Corresponding author.

E-mail address: [arh@jpl.nasa.gov](mailto:arh@jpl.nasa.gov) (A.R. Hendrix).

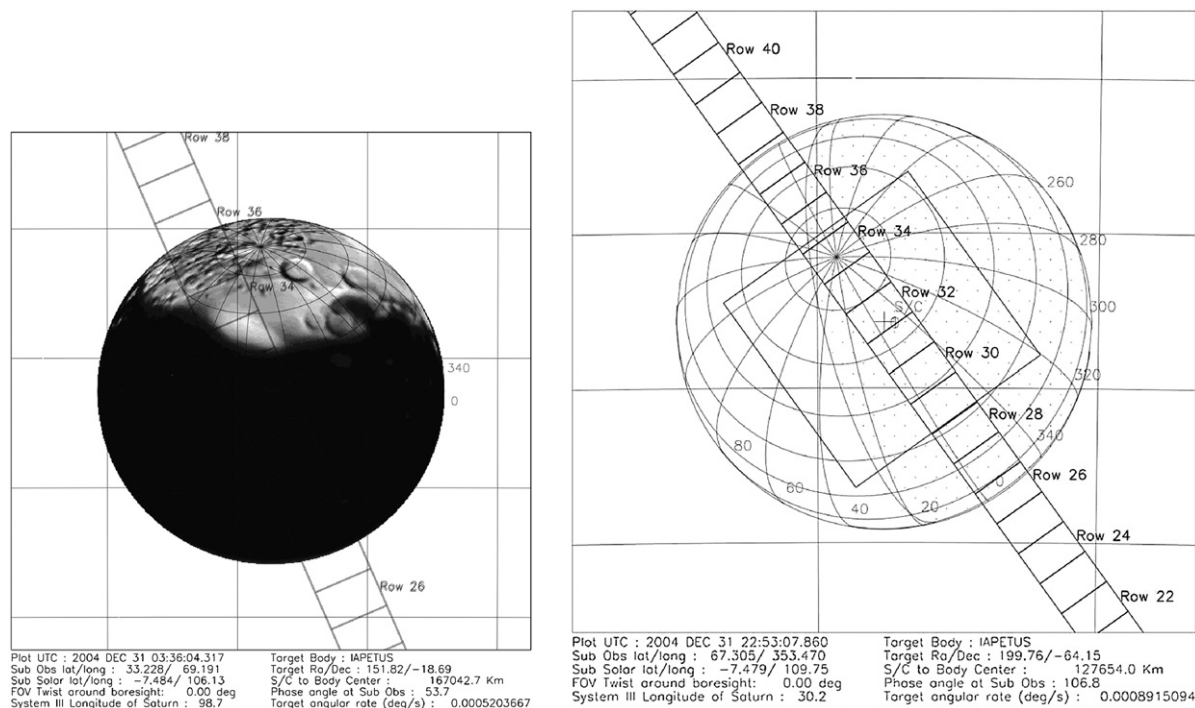


Fig. 1. Sample views of observational geometry near start of observations (left) and near end of observations (right). The location of the UVIS slit is also indicated, along with the relative size of the spatial pixels. The figure on the right also displays an ISS NAC field-of-view (FOV) for reference.

retrograde satellites exterior to Phoebe. However, it is likely that Phoebe would also be coated in the reddish dust (though not with the hemispheric pattern seen on Iapetus due to Phoebe's non-synchronous rotation)—but this does not appear to be the case.

Ground-based RADAR observations at 13 cm (Black et al., 2004) and Cassini RADAR data at 2.2 cm (Ostro et al., 2006) indicate that the dark terrain must be quite thin (one to several decimeters); an ammonia–water ice mixture may be present below several decimeters of the surface on both the leading and trailing hemispheres of Iapetus. The RADAR results appear to rule out the theories of a thick dark material layer (Matthews, 1992; Wilson and Sagan, 1996). Cassini Radio Science results (Rappaport et al., 2005) indicate a bulk density for Iapetus of  $1.1 \text{ g/cm}^3$ , from which it can be inferred that the moon is composed primarily of water ice. Because large craters within the dark terrain appear to be evenly colored with the dark material (no craters appear to break up the dark material, exposing bright underlying terrain), this suggests the emplacement of the dark material is relatively new or ongoing.

The exact composition of the dark material is not known; the presence of a deep  $3.0 \mu\text{m}$  absorption feature has led to comparisons with C-type asteroids (Lebofsky et al., 1982) and primitive meteorite-type material (Bell et al., 1984) while its red VNIR (visible-near infrared) spectrum has been compared with organic material (Cruikshank et al., 1983; Vilas et al., 1996). Water ice is present in very small amounts in the dark material; spectral mixing models (using both disk-integrated ground-based and disk-resolved Cassini data) show that the average dark terrain contains  $\sim 5\%$  water ice (Owen et al., 2001; Buratti et al., 2005b).

## 2. Observations and datasets

The observations reported here were obtained by the Cassini Ultraviolet Imaging Spectrograph (UVIS) (Esposito et al., 2004). The UVIS uses two-dimensional CODACON detectors to provide simultaneous spectral and one-dimensional spatial images. The second spatial dimension is acquired by slewing the UVIS slit across the target body. The far-UV channel of UVIS covers the  $1115\text{--}1912 \text{ \AA}$  range. The detector format is 1024 spectral pixels by 64 spatial pixels. Each spectral pixel is  $0.25 \text{ mrad}$  and each spatial pixel is  $1 \text{ mrad}$  projected on the sky. The high-resolution slit has a spectral resolution of  $2.75 \text{ \AA}$  and pixel width of  $0.75 \text{ mrad}$ . Iapetus measurements were made from a closest-approach distance of  $123,000 \text{ km}$  on December 31, 2004, of both the leading hemisphere dark terrain and the bright terrain in the north pole region. During the Iapetus flyby, Cassini flew over the leading, dark hemisphere which was illuminated at  $\sim 55^\circ\text{--}90^\circ$  phase. The groundtrack approached the northern hemisphere and went onto the unilluminated trailing hemisphere. Examples of observational geometry are shown in Fig. 1. The Iapetus observations used the low-resolution slit with a spectral resolution of  $4.8 \text{ \AA}$  and pixel width of  $1.5 \text{ mrad}$ . The Phoebe and Hyperion observations discussed in this report used the high-resolution slit.

## 3. Results

### 3.1. UV color variations with latitude and longitude

Color variations between Iapetus' dark and bright terrains, and within the dark terrain itself, are detected in UVIS images and spectra. Such color variations indicate compositional

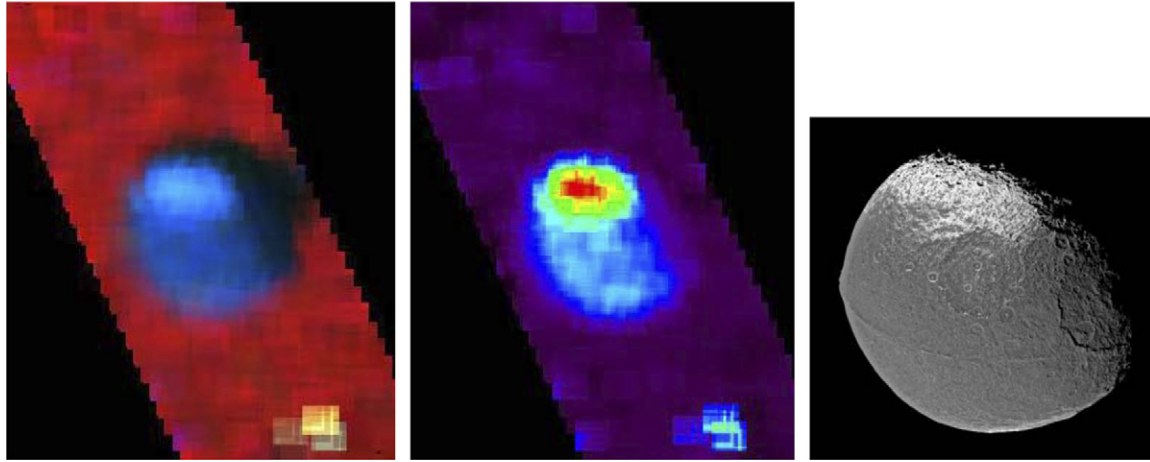


Fig. 2. (a) Three-color image of Iapetus. Red = Ly- $\alpha$  (1216 Å), blue-green = longer FUV wavelengths. Iapetus is darker than the Interplanetary Hydrogen (IPH) background at Ly- $\alpha$ . (b) Long-wavelength image of Iapetus. The leading hemisphere is dark, but not as dark as the unilluminated trailing hemisphere. A visible wavelength image with the same geometry is also shown.

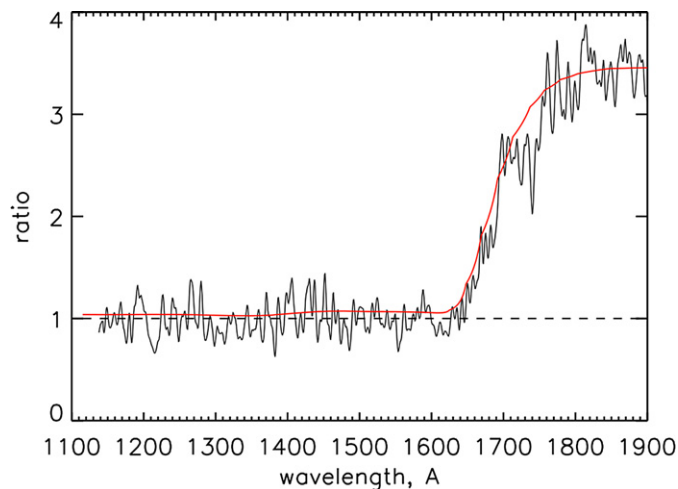


Fig. 3. Spectral ratio of bright terrain to average dark terrain, with a scaled model H<sub>2</sub>O ice reflectance spectrum overplotted. The ratio is very similar to pure water ice suggesting that the major difference between the two terrains is the amount of water ice present.

differences. UV images of Iapetus are shown in Fig. 2. Images are created by summing signal in three color bands: long-wavelengths (1800–1900 Å), mid-wavelengths (1600–1800 Å) and Ly- $\alpha$  (1216 Å). Iapetus is very dark at short FUV wavelengths (<1600 Å), and in fact reflects less light at Ly- $\alpha$  than is emitted by the surrounding Local Interstellar Medium, so it appears silhouetted against the sky background. Thus, UVIS detects the entire disk of Iapetus, though it is only partially illuminated by the Sun.

A plot of the average spectrum of Iapetus' bright terrain ratioed to the average dark terrain is shown in Fig. 3. The ratio spectrum is very similar to the reflectance spectrum of water ice (overplotted), suggesting that the major difference between the bright and dark terrains is that the bright terrain contains a higher amount of exposed water ice than the average dark terrain. Water ice has a very strong absorption feature at  $\sim$ 1600 Å (discussed also by Hendrix and Hansen, 2008).

To investigate albedo variations within the dark terrain, we subdivided the leading hemisphere into latitude/longitude bins. We distinguish between the apex region (centered on 90° W, between 45° and 135° W) and the non-apex regions (0°–45° W and 135°–180° W), for latitude bins 0°–10°, 10°–20°, 20°–30°, 30°–40° and >50° as shown in Fig. 4. We focus on the apex region where the signal was higher due to smaller phase angles.

We find that, in the apex region, there is little change in spectrum with latitude between 0° and 30° latitude. We thus bin together the spectra from these latitude regions for comparison with other regions. In the apex region, the 30°–40° latitude bin has a slightly stronger H<sub>2</sub>O ice band than the 0°–30° latitude bin, and the 40°–50° latitude bin of the apex region has a significantly stronger water ice absorption band than the 0°–30° region (Fig. 5). We can quantify the strength of the H<sub>2</sub>O ice band in each region by measuring the band depth  $D$ , where  $D = 1 - R_b/R_c$ ;  $R_b$  is the reflectance at the bottom of the absorption band (in this case, at shorter wavelengths, 1216–1335 Å) and  $R_c$  is the reflectance of the continuum, at longer wavelengths (1800–1900 Å). The 40°–50° latitude spectrum has a water ice band depth of 83% ( $\pm$ 6%) while the water ice band depth in the 30°–40° region is 73% ( $\pm$ 10%); the low latitude (0°–30°) region has a band depth of 50% ( $\pm$ 15%). In contrast, the bright polar region has a water ice band depth of 94% ( $\pm$ 2%). (These band depths could also be affected by the spectral shape of species other than water ice.) The H<sub>2</sub>O ice band depths are related to water ice abundance in the next section.

### 3.2. Comparisons with Phoebe and Hyperion

The possibility of Iapetus' dark material being related to Phoebe and/or Hyperion has been studied by many researchers at visible and near-IR wavelengths (e.g., Jarvis et al., 2000; Buratti et al., 2005a). We now extend that investigation to FUV wavelengths; Fig. 6 displays comparisons between the spectra of the bodies. Fig. 6a shows the spectra of Iapetus' bright and dark regions compared with the Phoebe average spectrum, all at

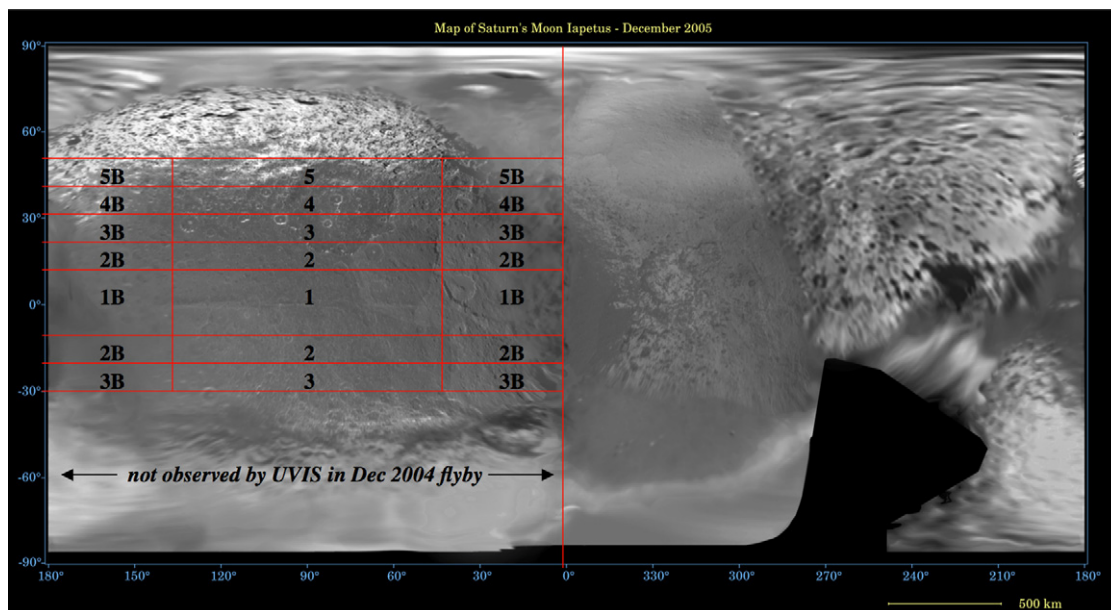


Fig. 4. Map showing the hemisphere of Iapetus observed by UVIS during the December 2004 Cassini flyby. The flyby focused on the northern leading hemisphere. The most southerly latitude observed by UVIS was  $\sim 28^\circ$  S, and the trailing hemisphere ( $180\text{--}360^\circ$  W) was not observed. The map shows the latitude–longitude bins used to analyze color variations within the dark material.

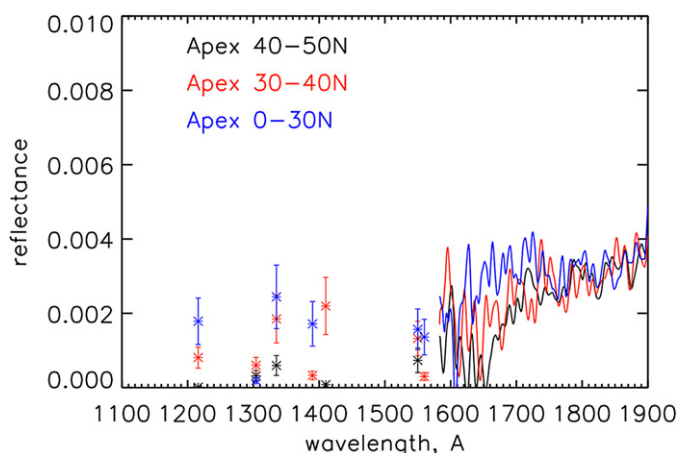


Fig. 5. Reflectance spectra in latitude bins of the apex longitude region ( $45^\circ\text{--}135^\circ$  W). Spectra have been scaled to the northernmost latitude spectrum at  $\sim 1850$  Å. Reflectance spectra are plotted as continua for wavelengths  $> 1600$  Å. Because both reflected signal and solar flux are low at wavelengths  $< 1600$  Å, the reflectance data are computed and plotted as points at wavelengths of solar emission feature, where sufficient reflected signal and solar flux exist. The  $0^\circ\text{--}30^\circ$  latitude region shows only a weak water ice band (55%) that is seen in the  $40^\circ\text{--}50^\circ$  latitude region (83%); the  $30^\circ\text{--}40^\circ$  latitude bin displays water ice band with a 73% depth. Also, the lower latitude spectra are relatively bright at short wavelengths, suggesting less water ice.

similar phase angles; the Phoebe spectrum does not agree with the Iapetus dark material spectrum—and in fact is much more spectrally similar to the spectrum of Iapetus’ bright terrain. The Iapetus bright terrain reflectance spectrum and the Hyperion average spectrum are very spectrally similar (Fig. 6b), though the Hyperion water ice band is slightly weaker (the slope of the upturn is not as steep). In Fig. 6b, the average Phoebe reflectance spectrum was determined using a smaller phase an-

gle, higher signal-to-noise spectrum than that shown in Fig. 6a, and scaled to the Iapetus bright terrain reflectance spectrum (from a larger phase angle); the greater signal-to-noise brings out the differences in the spectra of Phoebe and the Iapetus bright terrain. Phoebe is spectrally similar to Iapetus’ bright material, though Phoebe’s water ice band is weaker and Phoebe’s reflectance at the short FUV wavelengths is higher than that of the Iapetus bright terrain. The Iapetus dark terrain reflectance spectrum (Fig. 6c) has a weak  $\text{H}_2\text{O}$  band compared to the average Hyperion spectrum and compared to the Phoebe spectrum. It is thus very unlikely that pure Phoebe material or pure Hyperion material is what darkens Iapetus’ leading hemisphere, as suggested by previous researchers using Earth-based longer-wavelength datasets (e.g., Jarvis et al., 2000; Buratti et al., 2002). We do note, however, that at the longest FUV wavelengths Phoebe is darker than Hyperion and the Iapetus bright terrain, and is closer in spectral shape to the Iapetus dark terrain (Fig. 6c).

Because water ice is so dark at short FUV wavelengths, and is in fact generally darker than non-ice species (Fig. 7), the relative brightness of spectra in that wavelength region can be used to estimate relative amounts of water ice on a particular body or region. From the water ice absorption band depths shown in Figs. 6b and 6c, we can estimate that Iapetus’ bright regions have the most water ice, followed by Hyperion, Phoebe and the Iapetus dark terrain (in that order). This is also generally consistent with the visible geometric albedos of these bodies: the geometric albedos are  $\sim 0.4$ ,  $\sim 0.22$ , 0.08, and 0.04, for Iapetus’ bright terrain (Buratti et al., 2005b), Hyperion (Thomas and Veverka, 1985), Phoebe (Bauer et al., 2004) and Iapetus’ dark terrain (Buratti et al., 2005b), respectively.

We can use intimate mixtures models (after Roush, 1994) to investigate spectral differences within Iapetus’ terrains and

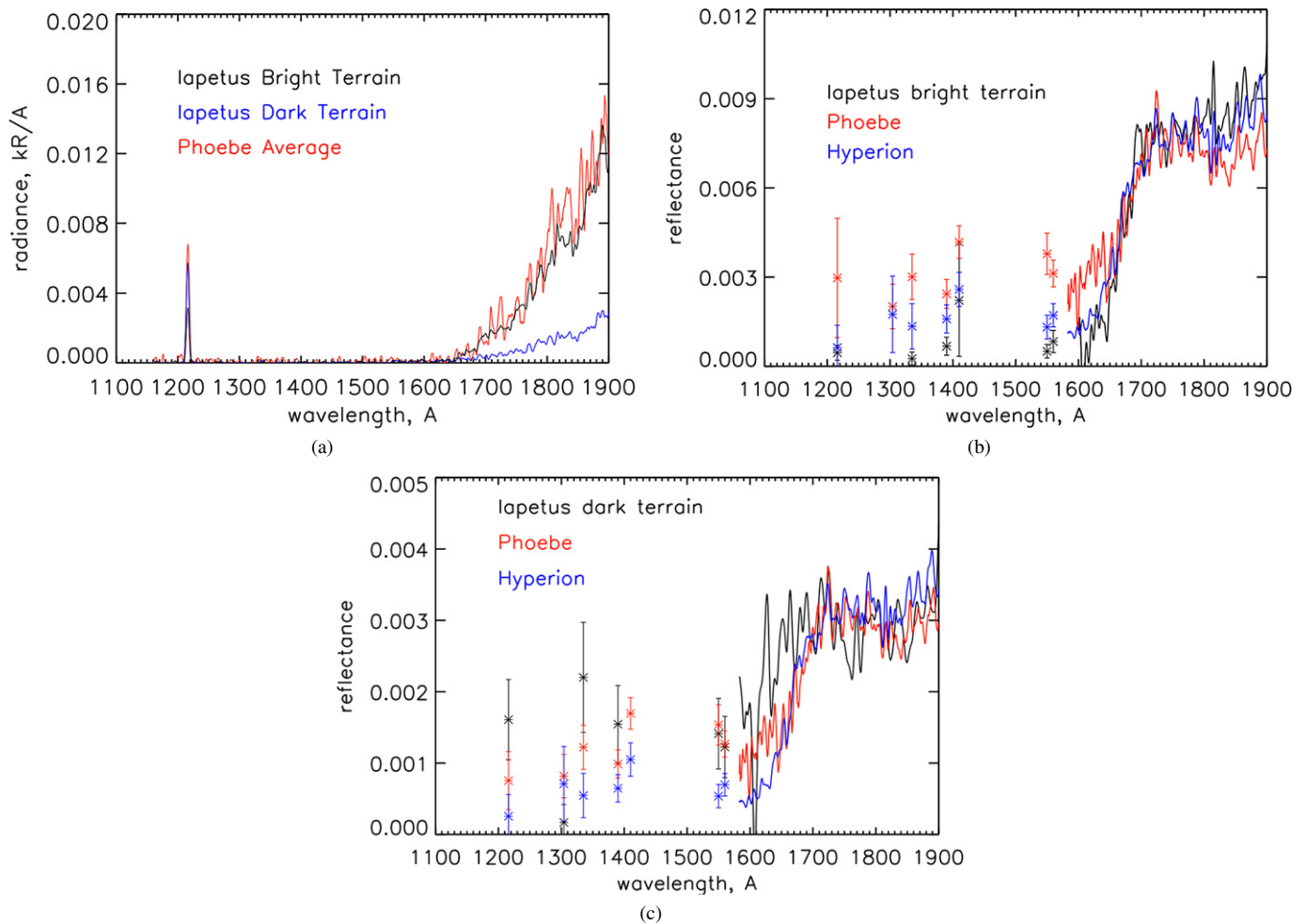


Fig. 6. (a) Average Phoebe radiance spectrum compared with average spectra of Iapetus' dark and bright terrains; all spectra were taken at similar phase angles. The Phoebe spectrum is very similar to the spectrum of the Iapetus bright material, and is very different from the spectrum of the Iapetus dark material. (b) Average Hyperion and average Phoebe reflectance spectra compared with Iapetus bright terrain reflectance spectrum. (Hyperion and Phoebe spectra are scaled to Iapetus spectrum at  $\sim 1730$  Å.) The spectra are similar, but the Phoebe spectrum is brighter than the others at short FUV wavelengths, and somewhat darker at the longest wavelengths; the water ice absorption feature is weaker. Hyperion and Iapetus bright material reflectance spectra are very similar, but the Hyperion water ice feature is slightly weaker than in the Iapetus bright terrain. (c) Average Hyperion and average Phoebe reflectance spectra compared with Iapetus dark terrain (low latitude apex region) reflectance spectrum. (Hyperion and Phoebe spectra are scaled to Iapetus spectrum at  $\sim 1730$  Å.) The Phoebe and Hyperion spectra both display water ice bands that are much stronger than in the Iapetus dark terrain spectrum. Phoebe is darker at the longest wavelengths than Hyperion and the Iapetus bright terrain, and is closer in spectral shape to the Iapetus dark terrain.

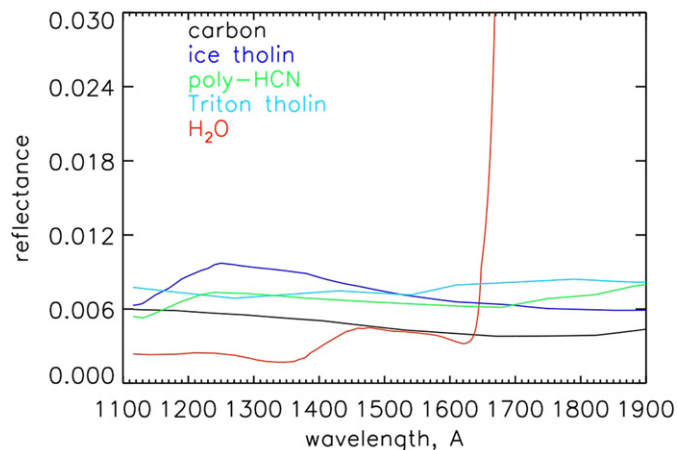


Fig. 7. Reflectance of water ice compared with reflectance spectra of Triton tholin and other non-ice species. Water ice is darker than these non-ice species at wavelengths shorter than  $\sim 1600$  Å.

between Iapetus, Phoebe and Hyperion. These Hapke models (Hapke, 1993) and procedures are discussed in application to UVIS data by Hendrix and Hansen (2008). We use water ice optical constants from Warren (1984) and optical constants for Triton tholin (after Cruikshank et al., 2005). Triton tholin is an organic solid made from the irradiation of a gas mixture of 0.999:0.001 N<sub>2</sub>:CH<sub>4</sub>; the empirical formula of the bulk substance is C<sub>3</sub>H<sub>5</sub>N<sub>4</sub> (McDonald et al., 1994). Buratti et al. (2005b) successfully modeled a Cassini VIMS spectrum (0.9–3.5  $\mu$ m) of the bright terrain of Iapetus using an intimate mixture of 78% water ice and 22% Triton tholin. We find that we can satisfactorily fit the UVIS spectrum of Iapetus's bright terrain using a very similar mixture (Fig. 8a).

The reflectance spectrum of the Iapetus bright terrain and the average Hyperion reflectance spectrum are very similar (Fig. 6b), but there are significant differences; the Hyperion water ice absorption feature is not as steep as that in the Iapetus

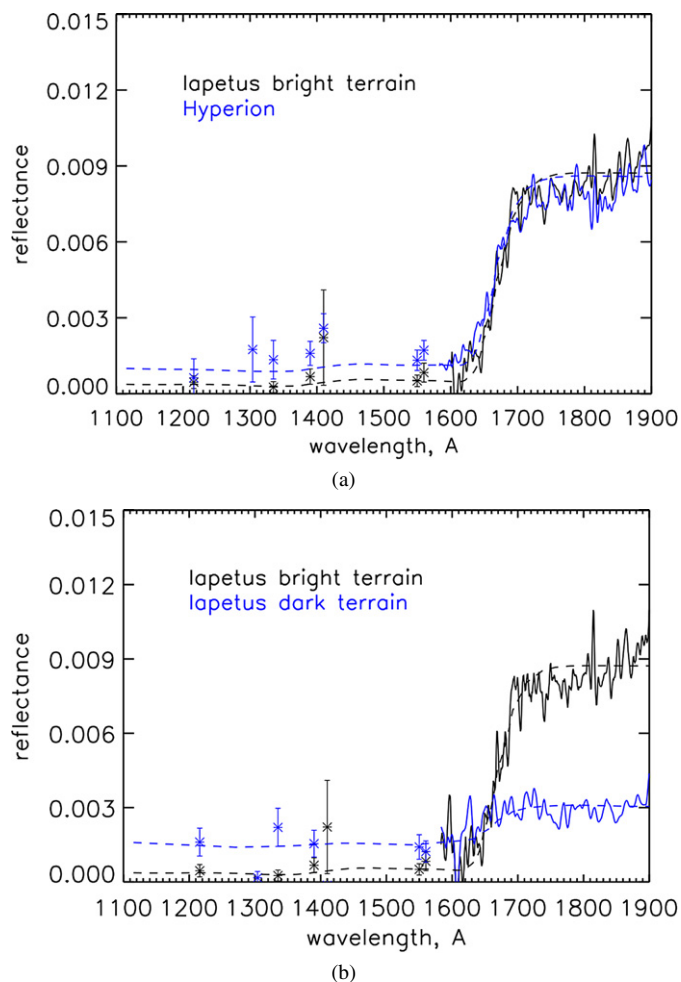


Fig. 8. (a) Model fits to Iapetus bright terrain and Hyperion average reflectance spectra (scaled). The reflectance spectrum of Iapetus' bright terrain can be fit with an intimate mixture of 75% H<sub>2</sub>O and 25% Triton tholin; the Hyperion spectrum is fit using 55% H<sub>2</sub>O ice and 45% Triton tholin. (b) The Iapetus dark terrain spectrum is fit with 5% H<sub>2</sub>O and 95% Triton tholin.

spectrum. We can fit the Hyperion spectrum with an intimate mixture model of 55% H<sub>2</sub>O ice and 45% Triton tholin (Fig. 8a). Similarly, the Phoebe reflectance spectrum can be fit with 10% H<sub>2</sub>O ice and 90% Triton tholin. We can estimate the amount of water ice within the dark terrain of Iapetus' leading hemisphere, in the latitude regions discussed above. We find that the low latitude apex region (0°–30° latitude, 45°–135° W longitude) can be fit with an intimate mixture of 5% water ice and 95% Triton tholin (Fig. 8b). The 30°–40° latitude bin can be fit using 15% water ice, while the 40°–50° region is well-fit using an intimate mixture model with 55% water ice and 45% Triton tholin. The water ice abundances are constrained to within ~3–5%. Previous researchers (Owen et al., 2001; Buratti et al., 2005b) modeled the *average* dark terrain with ~5% H<sub>2</sub>O ice plus dark materials. Here, we find ~5% H<sub>2</sub>O ice at just the lowest latitudes, with amount of water ice increasing with latitude. The differences are likely due to observational resolution and/or non-uniqueness of the Hapke models. What is important to stress here is that the UV H<sub>2</sub>O band is detected at the lowest latitudes, and the strength of the band increases with

latitude (Fig. 5). The Hapke model fits are not unique, but are consistent with the geometric albedos of these bodies.

Thus, in general, the UVIS spectra allow us to estimate water ice amounts, as a result of the strong water ice band at 1600 Å. Many of the candidate non-ice species are spectrally bland in this wavelength range and not particularly distinctive (Fig. 7). We find we can use the Triton tholin in varying amounts, along with water ice, to satisfactorily (although not uniquely) fit the spectra of Iapetus, Phoebe and Hyperion. Owen et al. (2001) used Triton tholin to model Iapetus' dark terrain spectrum and suggested that Titan is a possible source for the nitrogen-bearing material.

#### 4. Discussion

Iapetus' leading hemisphere is interesting not only because of the dark terrain, but because of the bright poles. The dark terrain pattern is consistent with an external impact source model (Cook and Franklin, 1970), which predicts bright poles. It has also been suggested that the poles are bright due to thermal segregation of water ice from the warmer low latitudes to the colder high latitudes (Spencer et al., 2005).

The fact that the dark material does not have a uniform amount of water ice, and that the water ice amount increases with latitude, has implications for the sources and processes. Assuming an exogenic source, with the bulk of the material coming in at the low latitude apex region (as predicted by Cook and Franklin, 1970), we can hypothesize that the spectrum measured near the apex is most consistent with the spectrum of the “pure” contaminant material—it should be the densest concentration of contaminant. (The material in this region is, however, most likely to also be altered by meteoritic bombardment.) Assuming for the moment the meteoritic bombardment does not play a role in altering the chemical nature of the material in the low-latitude apex region, our model results suggest that the incoming material has ~5% H<sub>2</sub>O ice.

Alternately, the “pure” contaminant material initially contained greater amounts of water ice, and the relatively warm temperatures [due in part to the slow rotation of Iapetus (Spencer et al., 2005)] caused the water to segregate to cooler temperatures at higher latitudes. If the incoming contaminant material originally had more water ice, this is consistent (considering for the moment only UVIS spectra) with either Hyperion or Phoebe dust as a source, since the UVIS spectra of both of those bodies are similar to the Iapetus dark terrain spectrum, but higher in water ice content. Our detection of increased amounts of water ice with latitude is consistent with a larger number of bright regions at higher latitudes, which act as cold traps for water ice moving to colder regions at higher latitudes. It is possible that our detection of water ice at the lowest latitudes in the apex region is due to exposed water ice, such as that seen at crater rims in the dark material at higher latitudes; however there is no sign of exposed water ice in ISS images at the best imaging resolution.

Cassini CIRS measurements (Spencer et al., 2005) show that the peak daytime temperature in Iapetus' dark terrain is ~130 K, implying that surface water ice is not stable there on

geological timescales. In this low latitude region, UVIS detects ~5% water ice. Moving north, in the 30°–40° latitude region, UVIS detects more water ice (~15%), where CIRS measured max daytime temperatures of ~115–120 K (Spencer et al., 2005). UVIS detects yet more water ice (~55%) in the 40°–50° region, where CIRS measures temperatures of ~110–115 K, and a greater amount of water ice (~75%) is estimated in the bright region north of 50° N latitude where max daytime temperatures are 110 K. The fact that we detect a small amount of water ice at low latitudes suggests an ongoing process, whereby water ice is still in the process of moving to high latitudes. The vapor pressure of water has been measured by Bryson et al. (1974) at temperatures from 131 to 187 K. They derive the vapor pressure equation:  $\ln P = \Delta H/RT + B$  with  $\Delta H = 11.4$  kcal/mol and  $B = 21.7$  in  $\ln(\text{Torr})$ . This gives a vapor pressure of  $1.8 \times 10^{-10}$  Torr at 130 K. These water molecules will migrate to cold traps. We extrapolate the vapor pressure equation to compare the vapor pressures at 110 K, which is  $5.91 \times 10^{-14}$  Torr, clearly many orders of magnitude lower. This difference will slowly remove water from equatorial regions to permanent cold traps at the poles. In order to quantify this movement of frost the Triton thermal model developed by Hansen and Paige (1992) has been modified to apply to water frost on Iapetus. This model takes into account seasonal temperature differences, and shows the migration of frost to the poles. So the water ice in the dark terrain may be there only temporarily, which could mean that we are detecting an ongoing process. Fig. 2 of Spencer (1987) shows that the thermal segregation time increases toward higher latitudes and toward higher albedos (the plot is for temperatures at the Galilean satellites but the overall idea is applicable here). On Iapetus, water ice may survive longer at high latitudes within the dark terrain because the surface albedo becomes higher with latitude (e.g., Squyres et al., 1984). The increase in albedo with latitude may be due to a greater percentage of the region being exposed water ice at crater rims; these regions also act as cold traps.

Thus, these results suggest that, if the dark material is exogenic, the darkening process may be a recent or ongoing activity. This is also supported by images of large basins and craters in the dark terrain, but with no bright material exposed (Porco et al., 2005), along with evidence from RADAR measurements that the dark material is a thin coating. Furthermore, Jarvis et al. (2000) point out that Iapetus' dark, red spectrum is suggestive of primitive, unaltered material. The relative "freshness" of Iapetus' dark, red material is consistent with the idea that organic-containing surfaces exposed to radiation eventually become darker and blacker (Andronico et al., 1987). Strazzulla (1986) suggests that Phoebe is so dark and gray because the outermost layers are carbonized by cosmic protons. Phoebe's underlying surface layers could be spectrally red, so that if micrometeoroid impacts produce dust that subsequently hits Iapetus, the dust could be red. However, Phoebe does not appear to exhibit any fresh, spectrally red-looking regions that would suggest a relatively recent cratering event.

Hyperion is spectrally red at visible wavelengths, similar to D-type asteroids, and has been compared with organic material (Jarvis et al., 2000). Buratti et al. (2002) find that Hyperion

and Iapetus dark material can be fit with similar models using reddish, D-type stuff, similar to the result obtained by Jarvis et al. (2000). Matthews (1992) argued that the Hyperion event (the destruction of the proto-Hyperion) did not occur very recently; but he also argued that the lack of craters in Iapetus' dark terrain argues for a thick layer of dark material. We now know that craters do exist within Cassini Regio, suggesting that the dark material has been relatively recently emplaced, or the emplacement is an ongoing process, and we also know from RADAR data (Black et al., 2004) that the dark material layer is thin. Thus, if the dark material on Iapetus is the result of the collision that disrupted Hyperion, then the Hyperion event occurred recently enough that its reddish spectrum has not been blackened/carbonized by radiation exposure. Considering just Hyperion and Phoebe as possible sources, the resultant dust and debris from the Hyperion event appears to be more consistent with the color and apparent timescale of the Iapetus dark material than does Phoebe dust.

## 5. Conclusions

UVIS-measured reflectance spectra of Iapetus have been presented. The diagnostic FUV water ice absorption band is present even in the low latitudes of the apex region of the dark leading hemisphere. The water ice band depth increases with latitude away from the apex. Comparisons with Phoebe and Hyperion show that both of those bodies are richer in water ice than the Iapetus dark terrain. If either of those bodies is the source of the Iapetus dark material, water ice has been lost in the impact process; or, perhaps a more likely scenario is that the water ice has been lost subsequent to impact on Iapetus. We consider the idea that the dark material is warm enough at low latitudes, partly due to the slow rotation of Iapetus (Spencer et al., 2005) that water ice has largely segregated from the lowest latitudes; the fact that water ice is present in the lowest, warmest latitudes suggests that the coating process is recent or ongoing. The idea that "fresher," less weathered organic material is reddish at VNIR wavelengths (Andronico et al., 1987) is further evidence for the recent or ongoing nature of the dark coating process. We suggest Hyperion as a more likely candidate for a darkening agent for Iapetus' dark material, compared to Phoebe. Phoebe's surface is dark and gray, with no sign of reddish (and thus younger) regions, whereas Hyperion's VNIR spectrum is reddish, suggesting a relatively young surface that has not yet been darkened by weathering. The event that disrupted Hyperion may have occurred relatively recently and the leftover water-rich, reddish debris continues to impact Iapetus. We present this scenario as a possibility; we cannot with just this dataset rule out other options, such as an endogenic source of the dark material, or the option that the water ice detected in the dark material is the result of transport from a water-rich subsurface layer.

## Acknowledgments

We are grateful for helpful conversations with Gary Hansen and James Bauer, and for helpful comments from Bob West and

Josh Colwell. Larry Esposito is the UVIS Principal Investigator. Tobias Owen and an anonymous reviewer provided thoughtful, constructive comments.

## References

- Andronico, G., Baratta, G.A., Spinella, F., Strazzulla, G., 1987. Optical evolution of laboratory-produced organics: Applications to Phoebe, Iapetus, outer belt asteroids and cometary nuclei. *Astron. Astrophys.* 184, 333–336.
- Bauer, J.M., Buratti, B.J., Simonelli, D.P., Owen Jr., W.M., 2004. Recovering the rotational light curve of Phoebe. *Astrophys. J.* 610, L57–L60.
- Bell, J.F., Cruikshank, D.P., Gaffey, M.J., 1984. The composition and origin of the Iapetus dark material. *Icarus* 61, 192–207.
- Black, G.J., Campbell, D.B., Carter, L.M., Ostro, S.J., 2004. Radar detection of Iapetus. *Science* 304, 553.
- Bryson, C.E., Cazcarra, V., Levenson, L.L., 1974. Sublimation rates and vapor pressures of H<sub>2</sub>O, CO<sub>2</sub>, N<sub>2</sub>O, and Xe. *J. Chem. Eng. Data* 19, 107–110.
- Buratti, B.J., Mosher, J.A., 1995. The dark side of Iapetus: Additional evidence for an exogenous origin. *Icarus* 115, 219–227.
- Buratti, B.J., Hicks, M.D., Tryka, K.A., Sittig, M.S., Newburn, R.L., 2002. High-resolution 0.33–0.92  $\mu\text{m}$  spectra of Iapetus, Hyperion, Phoebe, Rhea, Dione and D-type asteroids: How are they related? *Icarus* 155, 375–381.
- Buratti, B.J., Hicks, M.D., Davies, A., 2005a. Spectrophotometry of the small satellites of Saturn and their relationship to Iapetus, Phoebe, and Hyperion. *Icarus* 175, 490–495.
- Buratti, B.J., and 28 colleagues, 2005b. Cassini Visual and Infrared Mapping Spectrometer observations of Iapetus: Detection of CO<sub>2</sub>. *Astrophys. J.* 622, L149–L152.
- Burns, J.A., Lamy, P.L., Soter, S., 1979. Radiation forces on small particles in the Solar System. *Icarus* 40, 1–48.
- Cook, A.F., Franklin, F., 1970. An explanation for the light curve of Iapetus. *Icarus* 13, 282–291.
- Cruikshank, D.P., Bell, J.F., Gaffey, M.J., Brown, R.H., Howell, R., Beerman, C., Rognstad, M., 1983. The dark side of Iapetus. *Icarus* 53, 90–104.
- Cruikshank, D.P., Owen, T.C., Dalle Ore, C., Geballe, T.R., Roush, T.L., de Bergh, C., Sandford, S.A., Poulet, F., Benedix, G.K., Emery, J.P., 2005. A spectroscopic study of the surfaces of Saturn's large satellites: H<sub>2</sub>O ice, tholins and minor constituents. *Icarus* 175, 268–283.
- Esposito, L.W., et al., 2004. The Cassini ultraviolet imaging spectrograph investigation. *Space Sci. Rev.* 115, 299–361.
- Hansen, C.J., Paige, D.A., 1992. A thermal model for the seasonal nitrogen cycle on Triton. *Icarus* 99, 273–288.
- Hapke, B., 1993. *Theory of Reflectance and Emittance Spectroscopy*. Cambridge Univ. Press, New York.
- Hendrix, A.R., Hansen, C.J., 2008. Ultraviolet observations of Phoebe from the Cassini UVIS. *Icarus* 93, 323–333.
- Jarvis, K.S., Vilas, F., Larson, S.M., Gaffey, M.J., 2000. Are Hyperion and Phoebe linked to Iapetus? *Icarus* 146, 125–132.
- Lebofsky, L.A., Feierberg, M.A., Tokunaga, A.T., 1982. Infrared observations of the dark side of Iapetus. *Icarus* 49, 382–386.
- Matthews, R.A.J., 1992. The darkening of Iapetus and the origin of Hyperion. *Q. J. R. Astron. Soc.* 33, 253–258.
- McDonald, G.D., Thompson, W.R., Heinrich, M., Khare, B.N., Sagan, C., 1994. Chemical investigation of Titan and Triton tholins. *Icarus* 108, 137–145.
- Ostro, S.J., and 19 colleagues, 2006. Cassini RADAR observations of Enceladus, Tethys, Dione, Rhea, Iapetus, Hyperion, and Phoebe. *Icarus* 183, 479–490.
- Owen, T.C., Cruikshank, D.P., Dalle Ore, C.M., Geballe, T.R., Roush, T.L., de Bergh, C., Meier, R., Pendleton, Y.J., Khare, B.N., 2001. Decoding the domino: The dark side of Iapetus. *Icarus* 149, 160–172.
- Porco, C.C., and 34 colleagues, 2005. Cassini imaging science: Initial results on Phoebe and Iapetus. *Science* 307, 1237–1242.
- Rappaport, N.J., Iess, L., Tortora, P., Asmar, S.W., Somenzi, L., Anabtawi, A., Barbinis, E., Fleischman, D.U., Goltz, G.L., 2005. Gravity science in the saturnian system: The masses of Phoebe, Iapetus, Dione, and Enceladus. *Bull. Am. Astron. Soc.* 37, 704.
- Roush, T.L., 1994. Charon: More than water ice? *Icarus* 108, 243–254.
- Smith, B.A., and 26 colleagues, 1981. Encounter with Saturn: Voyager 1 imaging science results. *Science* 212, 163–191.
- Smith, B.A., and 28 colleagues, 1982. A new look at the Saturn system: The Voyager 2 images. *Science* 215, 504–537.
- Soter, S., 1974. Brightness of Iapetus. Presented at IAU Colloq. 28, Cornell Univ.
- Spencer, J.R., 1987. Thermal segregation of water ice on the Galilean satellites. *Icarus* 69, 297–313.
- Spencer, J.R., Pearl, J.C., Segura, M., and Cassini CIRS Team, 2005. Cassini CIRS observations of Iapetus' thermal emission. *Lunar Planet. Sci. XXXVI*. Abstract.
- Squyres, S.W., Buratti, B., Veverka, J., Sagan, C., 1984. Voyager photometry of Iapetus. *Icarus* 59, 426–435.
- Strazzulla, G., 1986. Organic material from Phoebe to Iapetus. *Icarus* 66, 397–400.
- Thomas, P., Veverka, J., 1985. Hyperion: Analysis of Voyager observations. *Icarus* 64, 414–424.
- Vilas, F., Larson, S.M., Stockstill, K.R., Gaffey, J.J., 1996. Unraveling the zebra: Clues to the Iapetus dark material composition. *Icarus* 124, 262–267.
- Warren, S.G., 1984. Optical constants of ice from the ultraviolet to the microwave. *Appl. Opt.* 23, 1206–1225.
- Wilson, P.D., Sagan, C., 1995. Spectrophotometry and organic matter on Iapetus. 1. Composition models. *J. Geophys. Res.* 100, 7531–7537.
- Wilson, P.D., Sagan, C., 1996. Spectrophotometry and organic matter on Iapetus. 2. Models of interhemispheric asymmetry. *Icarus* 122, 92–106.